Reynolds Number Effects on the Steady and Unsteady Aerodynamic Forces Acting on the Bridge Deck Sections of Long-Span Suspension Bridge

MATSUDA Kazutoshi : Dr. Eng., P. Eng., Manager, Heat and Fluid Dynamics Department, Research Laboratory, Research & Development
TOKUSHIGE Masafumi : Design Dept., Bridge & Road Construction Division, Logistics Systems & Structures
IWASAKI Tooru : Engineering, Galaxy Express Corporation

This paper gives the results of research on Reynolds number effects on steady and unsteady aerodynamic forces on twin-box bridge section models of different scales in three different wind tunnels. The forces were measured over a wide Reynolds number range from 1.1×10^4 to 1.5×10^6 based on the dimension of deck height. In order to investigate Reynolds number effects on the steady and the unsteady aerodynamic forces, wind-induced static displacement analysis and flutter analysis were carried out for a suspension bridge with a main span of 2 500 m using a three-dimensional analytical model. Also, the paper considers amplitude effects on both the unsteady aerodynamic forces and the predicted flutter speeds.

1. Introduction

The 1940 collapse accident of "the Tacoma Narrows Bridge" in the United States triggered the recognition of the importance of dynamic wind effect in the wind resistant design of a bridge for the first time. Since then, a check by a wind tunnel test has come to be done to ensure the aerodynamic stability of a long-span bridge. If a wind tunnel test is to be done using a wind tunnel of low wind speed, the aeroelastic similarity conditions must be made equal between the real phenomenon and the wind tunnel test. One such condition is Reynolds number, which is the ratio of inertial force to viscous force of a fluid; however, it is difficult to achieve equality in ordinary cases. In a full bridge model wind tunnel test using a full aerostatic model, take a model scale of, for example, 1/50 to 1/150 and assume that the aeroelastic similarity based on Froude number is satisfied. Then the ratio of Reynolds number between the real bridge and wind tunnel test ranges from 354 ($=50 \times \sqrt{50}$) to 1 837 ($=150 \times \sqrt{150}$), that is, there is a difference of the order of 10^2 to 10^3. Therefore, in wind tunnel tests of a long-span bridge or other large steel structure, the test conditions are set ignoring the similarity with respect to Reynolds number. When wind acts on a bridge or other bluff structure, the separation point of the flow is thought to be fixed. In practice, therefore, wind tunnels tests have been performed assuming that Reynolds number has little influence on the wind resistance of the structure.

Recently, however, there are an increasing number of cases reported in Refs[1] - [5] on the wind tunnel test of a bridge in which the aerodynamic characteristics or wind response is influenced by Reynolds number. If the aerodynamic characteristics or wind response differs for different Reynolds numbers, there is a risk of erring in the estimation or evaluation of the response of a real bridge to wind. Therefore, it is important for the wind resistant design of a long-span bridge to understand Reynolds number effects on wind tunnel test results.

Using three different wind tunnels and bridge deck models, this study measured the steady and unsteady aerodynamic forces acting on the bridge deck model in Reynolds number range from 1.1×10^4 to 1.5×10^6 (representative length: deck height) and looked at Reynolds number effects on each type of aerodynamic forces. As a study case in the past using a bridge deck model in a high Reynolds number region, there are steady aerodynamic force measurements[3] and spring-supported model tests.[4], [5] In this study, not only steady aerodynamic force, but also unsteady aerodynamic force obtained by the forced excitation method, was measured. Unsteady aerodynamic force measurement was made in a high Reynolds number region that was smaller by a factor of 10^1 than that of the real bridge, and this was the world's first attempt. Further, the obtained steady and unsteady aerodynamic force coefficients were applied to a three-dimensional analysis model of a long-span suspension bridge having a center span of 2 500 meters to investigate Reynolds number effects on the wind-induced static displacements and flutter wind speed of the real bridge. Results are also reported here. Flutter in this study means coupled flutter, which is a self-excited vibration consisting

of a vertical bending motion and torsional motion coupled with a phase difference.

2. Wind Tunnel Test

From the definition equation of Reynolds number shown by Equation (1), one can see that a higher Reynolds number can be ensured for a higher mean wind speed and a larger model.

$$Re = \frac{VD}{\nu} \quad \cdots\cdots (1)$$

where

Re : Reynolds number
V : Mean wind speed (m/s)
D : Representative length, or deck height in this case (m)
ν : Kinematic viscosity coefficient (m^2/s)

Therefore, this study used bridge deck models of different sizes and wind tunnels corresponding to them in size in order to measure steady and unsteady aerodynamic forces in a wide range of Reynolds numbers while ensuring high Reynolds numbers. For the model scale, 1/10, 1/30 and 1/80 were employed considering the test section size of the wind tunnels used. These three models have the same cross-sectional shape. The three wind tunnels and models are shown in **Figs. 1** to **3**. A cross-sectional view of the bridge deck under study is shown in **Fig. 4**. **Table 1** shows the major dimensions of the bridge deck models. The steady and unsteady aerodynamic forces acting on the model were measured using load cells set at both ends of and inside the model. In addition, a combined total of 60 pressure holes were provided on the upstream and downstream halves of the deck to measure the surface pressure distribution around the model cross-section. The definition equations of mean and fluctuating pressure coefficients are shown in Equations (2) and (3).

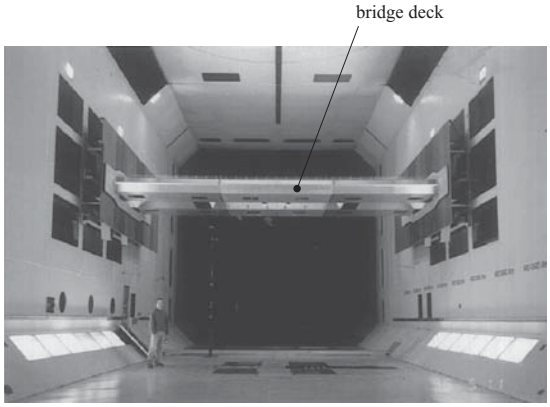

(Note) *1 : National Research Council Canada

Fig. 1 1/10 scale bridge deck model mounted in the NRC*1 9.1 m × 9.1 m wind tunnel

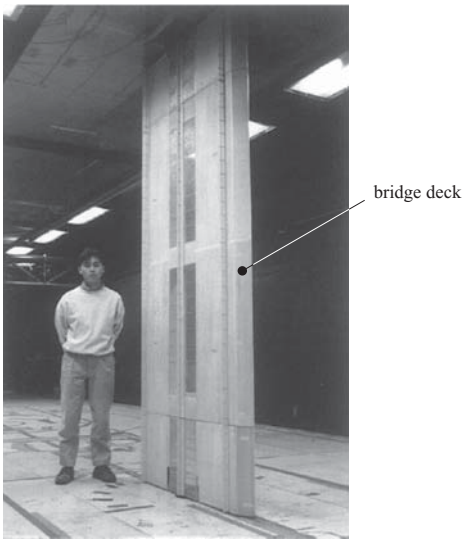

Fig. 2 1/30 scale bridge deck model mounted in the IHI 6 m × 3 m wind tunnel

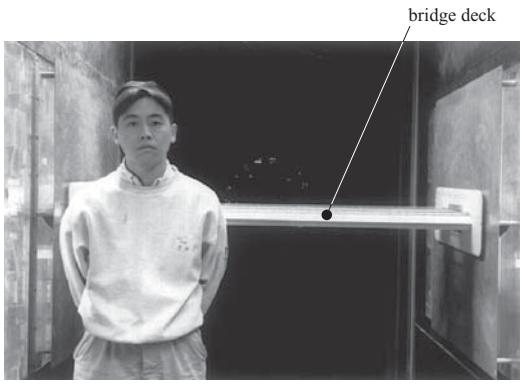

Fig. 3 1/80 scale bridge deck model mounted in the IHI 1.5 m × 2.5 m wind tunnel

$$C_{PS} = \frac{P_S - P_0}{\frac{1}{2}\rho V^2} \quad \cdots\cdots (2)$$

$$C_{PD} = \frac{P_D}{\frac{1}{2}\rho V^2} \quad \cdots\cdots (3)$$

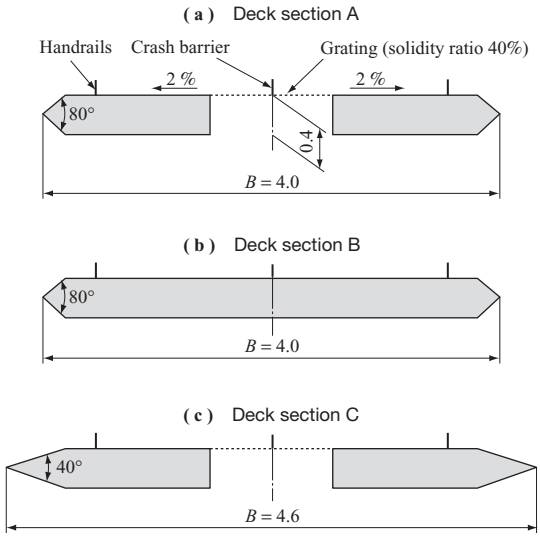

(Note) Dimensions are values of a 1/10 scale bridge deck model.

Fig. 4 Bridge deck cross section (unit: m)

where

C_{PS} : Mean pressure coefficient
C_{PD} : Fluctuating pressure coefficient
P_S : Mean pressure (= Total pressure) (N/m^2)
P_0 : Reference static pressure (N/m^2)
P_D : RMS value of fluctuating pressure (N/m^2)
ρ : Air density (kg/m^3)
V : Mean wind speed (m/s)

Table 2 shows the major dimensions and Reynolds number range of the wind tunnels used. To ensure high Reynolds numbers, the large wind tunnel of the National Research Council Canada (NRC) was used. The test section size is 9.1 meters wide by 9.1 meters high by 23.9 meters long, and the maximum wind speed is 55 meters per second. For the airflow in the wind tunnels, a smooth flow with small turbulence intensity was employed in every case.

In addition, Strouhal number was calculated by measuring the frequency of the shed vortex street generated in the wake area of the bridge deck model. The frequency of a shed vortex street is in proportion to the wind speed and in inverse proportion to the representative length of the structure. As shown by Equation (4), the Strouhal number is defined as the proportionality constant and is a dimensionless number specific to the cross-sectional shape of the structure.

$$St = \frac{fD}{V} \quad \cdots\cdots (4)$$

where

St : Strouhal number (—)
f : Vortex shedding frequency (1/s)
D : Deck height (m)
V : Mean wind speed (m/s)

3. Reynolds number effects on aerodynamic forces acting on bridge deck

3.1 Steady aerodynamic forces

3.1.1 Relationship between Reynolds number and steady aerodynamic coefficients

The steady aerodynamic forces are the time mean components of the aerodynamic forces acting on the bridge deck and can be classified into the three force components of drag, lift and pitching moment as shown in **Fig. 5**. When rendered dimensionless, they are called the drag coefficient, lift coefficient and moment coefficient, respectively, and expressed as the following definition equations:

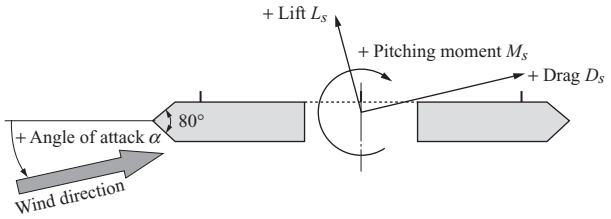

Fig. 5 Steady aerodynamic force

$$C_D = \frac{D_S}{\frac{1}{2}\rho V^2 A_n} \quad \cdots\cdots (5)$$

$$C_L = \frac{L_S}{\frac{1}{2}\rho V^2 B} \quad \cdots\cdots (6)$$

$$C_M = \frac{M_S}{\frac{1}{2}\rho V^2 B^2} \quad \cdots\cdots (7)$$

where

C_D : Drag coefficient
C_L : Lift coefficient
C_M : Pitching moment coefficient
D_S : Mean drag per unit length (N/m)
L_S : Mean lift per unit length (N/m)
M_S : Mean pitching moment per unit length (N·m/m)
ρ : Air density (kg/m^3)
V : Mean wind speed (m/s)
A_n : Projected area per unit length of bridge deck, or value of deck height only of real bridge in this case (= 4 m^2/m)
B : Value of deck width of real bridge (= 40 m)

The steady aerodynamic force coefficients at Deck sections A, B and C shown in **Fig. 4** are shown in **Figs. 6**, **7** and **8**, respectively. Reynolds number effects on the steady aerodynamic force coefficients were conspicuous at Deck section A in **Fig. 6**. At angles of attack below −2 degrees and above +3 degrees, the lift and pitching moment coefficients change as the Reynolds number

Table 1 Bridge deck cross section model properties

Scale	Total width B (m)	Height H (m)	Length L (m)	Aspect ratio L/B
1/10	4.0	0.4	8.0	2.0
1/30	1.3	0.13	3.0	2.3
1/80	0.5	0.05	1.35	2.7

Table 2 Wind tunnel properties

Wind tunnel	Test section			Wind speed range (m/s)	Reynolds number range $Re = VD/\nu$
	Width (m)	Height (m)	Length (m)		
the NRC 9.1 m × 9.1 m wind tunnel	9.1	9.1	23.9	5 - 55	1.4×10^5 - 1.5×10^6
the IHI 6 m × 3 m wind tunnel	6.0	3.0	24.0	0.5 - 15	4.5×10^3 - 1.4×10^5
the IHI 1.5 m × 2.5 m wind tunnel	1.5	2.5	8.0	0.5 - 20	1.7×10^3 - 6.8×10^4

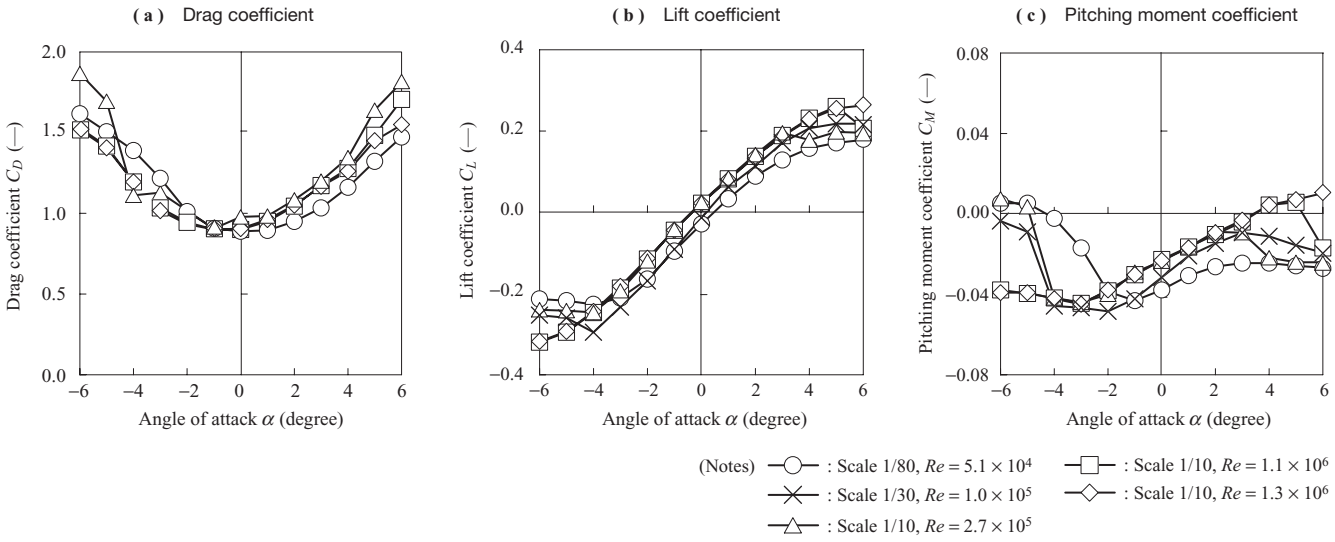

Fig. 6 Relationship between angle of attack and steady aerodynamic force coefficients (Deck section A)

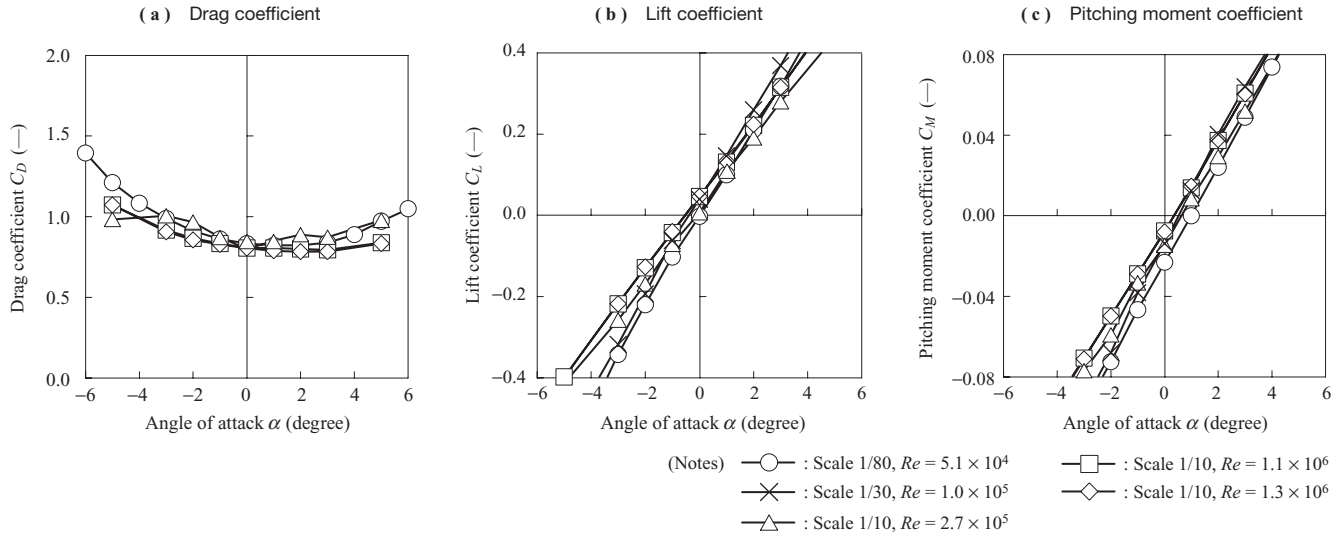

Fig. 7 Relationship between angle of attack and steady aerodynamic force coefficients (Deck section B)

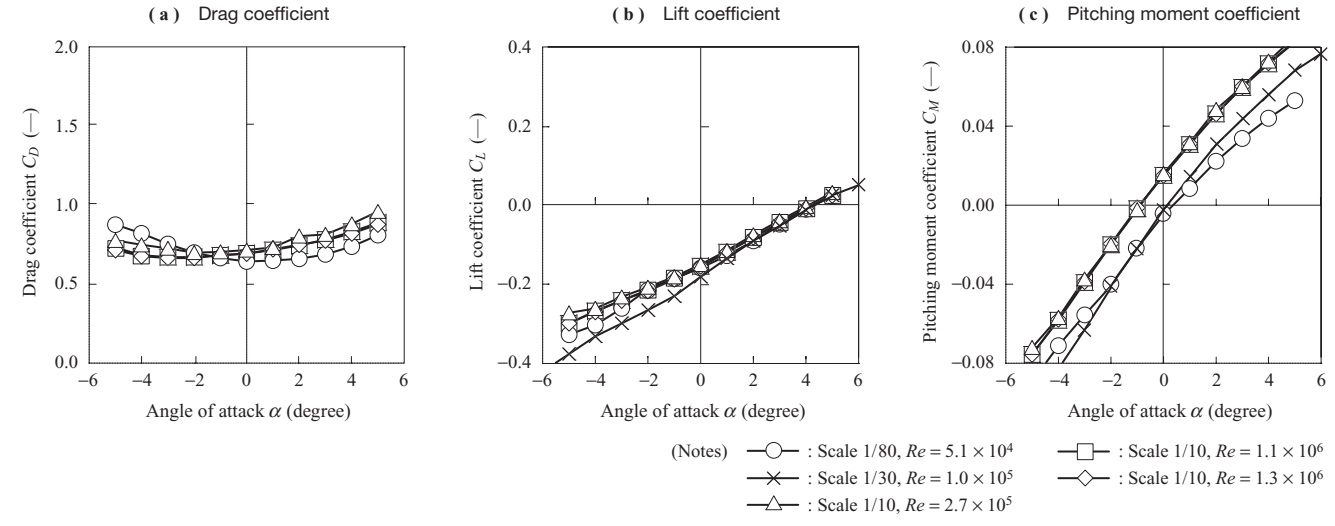

Fig. 8 Relationship between angle of attack and steady aerodynamic force coefficients (Deck section C)

increases. At angles of attack near 0 degree, these coefficients change a little with the Reynolds number. This tendency at an angle of attack of 0 degree is similar to the steady aerodynamic force coefficients of a 1/10 scale model[3] of "the Normandy Bridge" in France. The measured Reynolds number range at this time is, taking the deck height as the representative length, from 0.2×10^6 to 1.7×10^6.

3.1.2 Mechanism of Reynolds number effects on steady aerodynamic forces

The lift and pitching moment coefficients at Deck section A are influenced by Reynolds numbers at angles of attack below −2 degrees and above +3 degrees. The mechanism for this is looked at here from the measured results of pressure distribution at the model surface. The mean pressure distribution at the model surface in Deck section A at rest is shown in **Fig. 9** for angles of attack of −5, 0 and +5 degrees. At all the angles of attack, the pressure distribution locally changes at the top and bottom surfaces of the upstream deck half as the Reynolds number increases. At an angle of attack of −5 degrees, for example, as the Reynolds number increases, the magnitude of the negative pressure at the bottom surface of the upstream deck half increases, so the downward lift and negative steady aerodynamic pitching moment increase. Therefore, the lift and pitching moment coefficients at an angle of attack of −5 degrees in **Fig. 6** can be thought to increase in magnitude, but in the negative direction, as the Reynolds number increases.

At an angle of attack of +5 degrees, as the Reynolds number increases, the magnitude of the negative pressure at the bottom surface of the upstream deck half decreases and the magnitude of the negative pressure at the top surface of the upstream deck half increases, so the upward lift and positive pitching moment increase. As a result, with increasing Reynolds number, the lift coefficient at an angle of attack of +5 degrees shown in **Fig. 6** can be thought to increase in magnitude in the positive direction, and the pitching moment coefficient can be thought to change from negative to positive.

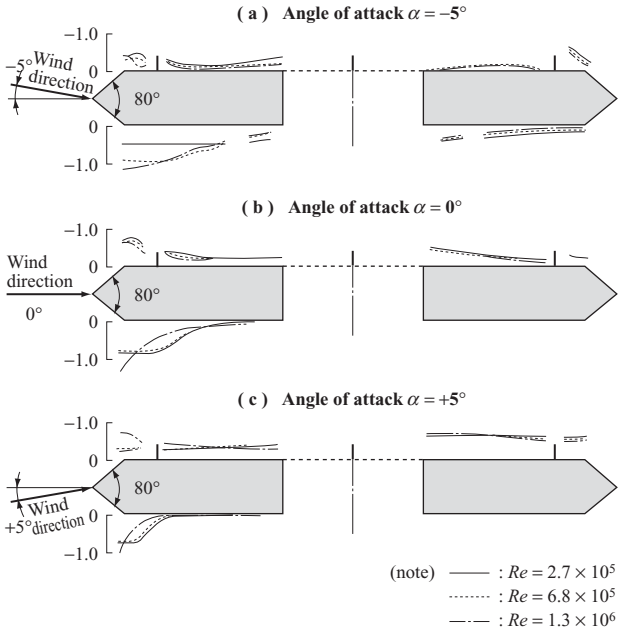

Fig. 9 Surface pressure distribution (Deck section A)

At any angle of attack, the peak of the negative pressure at the bottom surface end of the upstream deck half shifts to the upstream side as the Reynolds number increases. This tendency is also seen in past studies on an inverted trapezoidal-shaped deck section[6] and π-shaped deck section of a cable-stayed bridge.[7]

3.1.3 Relationship between drag coefficient and Strouhal number

A representative example in which Strouhal number is influenced by Reynolds number is a cylindrical section. That is, the Strouhal number is about 0.2 in the subcritical region and a critical region with the Reynolds number of about 3×10^5 or less, while it is as large as about 0.5 in a higher critical region and the supercritical region.[8]-[10] In this way the Strouhal number increases with the Reynolds number, and this means from Equation (4) that the rate of increase of vortex shedding frequency is higher than the rate of increase of wind speed, namely, the width of the shed vortices generated in the wake area of the bridge deck model becomes narrow.

In past studies, Shu et al.[11] measured the Strouhal number of rectangular sections with B/D = 2, 4 and 6 (B: Deck width, D: Deck height) and pointed out as a result that with a large aspect ratio with B/D, the Reynolds number has a large influence on the Strouhal number when the Reynolds number is 5 000 or less. They concluded that a 1-box cross section showed a similar tendency to a rectangular section. Schewe et al.[2] ascertained Reynolds number effects on the steady aerodynamic force coefficients for an inverted trapezoidal cross-section and say that, for such a cross-section, the relationship between the Strouhal number St and drag coefficient C_D can be expressed as Equation (8).

$$St \times C_D = \text{Constant} \quad \cdots\cdots (8)$$

The relationship between drag coefficient and Strouhal number at Deck section A, where Reynolds number effects were observed, is shown in **Fig. 10**. At angles of attack of −5 and +5 degrees, the Strouhal number increases, while the drag coefficient decreases as the Reynolds number increases. At an angle of attack of 0 degree, Reynolds number effects were hardly observed, even for the same section, so the Strouhal number and drag coefficient were not influenced by the Reynolds number and almost constant. **Figure 11** shows the relationship between the Reynolds number and $St \times C_D$. As with the past research results, it was verified that Equation (8) holds true also for Deck section A. Therefore, it was found that the Reynolds number effects on the drag coefficient can also be explained from the viewpoint of the Strouhal number.

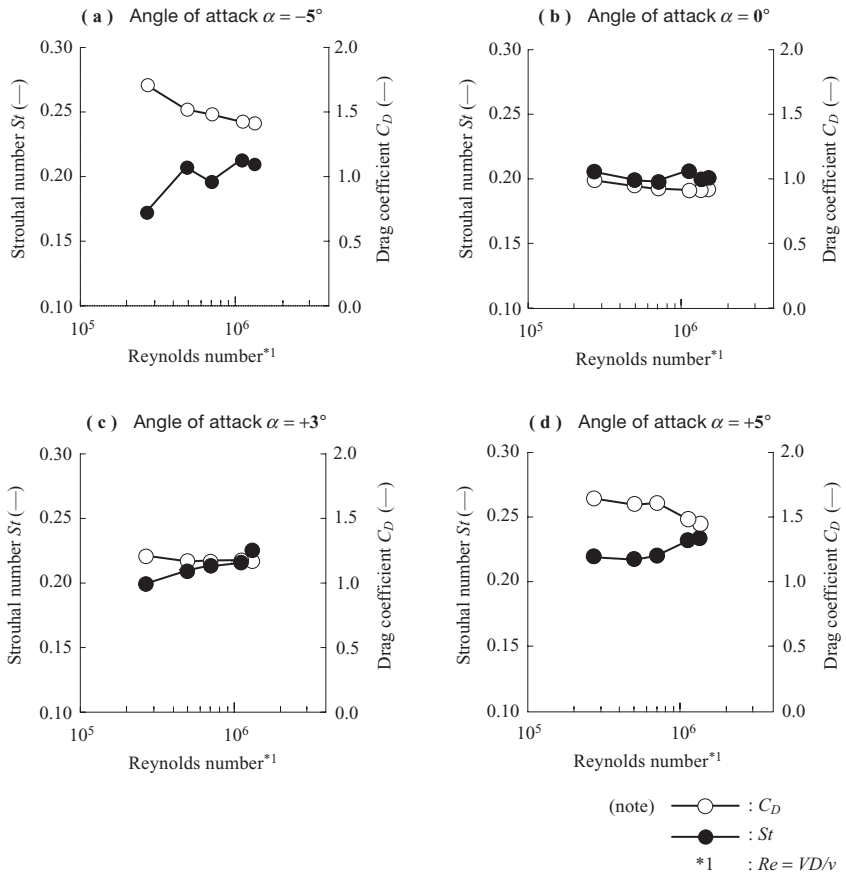

Fig. 10 Relationship between drag coefficients and Strouhal numbers (Deck section A)

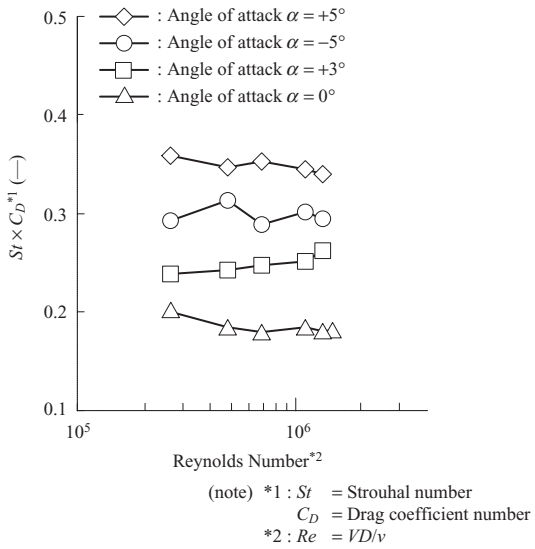

Fig. 11 Relationship between Reynolds number and $St \times C_D$ (Deck section A)

3.2 Unsteady aerodynamic forces

3.2.1 Outline of unsteady aerodynamic forces

When examining the flutter characteristics of a long-span bridge, the most reliable technique will be, judging from the current technical level, a full bridge model test using a full aerostatic model. However, the Reynolds number of a wind tunnel test is smaller by a factor of 10^2 to 10^3 than that of a real bridge, so the aeroelastic similarity condition with respect to the Reynolds number cannot be satisfied in ordinary cases. The test expenses are high, including the model fabrication cost, and the test has trouble with a parametric study of bridge deck section shape. For these and other reasons, employment of this technique is sometimes shelved.

In a technique replacing this full bridge model test, the unsteady aerodynamic forces acting on the bridge deck model are found by a wind tunnel test, then the obtained aerodynamic forces are input as external forces of the equations of motion of the whole bridge system, and the flutter characteristics are estimated by a flutter analysis program in an analytical way. This section pays attention to the unsteady aerodynamic forces used in this method. The unsteady aerodynamic forces can be transformed into dimensionless unsteady aerodynamic force coefficients, which depend on the cross-sectional shape, Reynolds number, reduced frequency, angle of attack and amplitude in ordinary cases. Of these, there are few investigations into the effects of the Reynolds number.

In 1950, when Bleich[12] investigated the causes for "the Tacoma Narrows Bridge" collapse accident, he applied the unsteady aerodynamic forces acting on the plate wing as thought out by Theodorsen[13] and pointed

out the possibility of flutter in a suspension bridge with a truss stiffening girder. When a two-dimensional plate rigid wing is in harmonic oscillation with two degrees of freedom of vertical bending and torsion of small constant amplitude, the unsteady lift and unsteady pitching moment acting on this wing can be expressed by the following equations:

$$L=-\pi\rho b^2\left\{\ddot{\eta}+V\dot{\theta}-ba\ddot{\theta}\right\} -2\pi\rho VbC(k)\left\{\dot{\eta}+V\theta+b\left(\frac{1}{2}-a\right)\dot{\theta}\right\} \quad \cdots\cdots (9)$$

$$M=\pi\rho b^3\left\{a\ddot{\eta}-V\left(\frac{1}{2}-a\right)\dot{\theta}-b\left(\frac{1}{8}+a^2\right)\ddot{\theta}\right\} +2\pi\rho Vb^2\left(a+\frac{1}{2}\right)C(k)\left\{\dot{\eta}+V\theta+b\left(\frac{1}{2}-a\right)\dot{\theta}\right\} \quad \cdots (10)$$

where

L : Unsteady lift (downward is positive) (N/m)
M : Unsteady pitching moment (pitch-up is positive) (N·m/m)
ρ : Air density (kg/m^3)
b : Half chord length (m)
V : Mean wind speed (m/s)
a : See **Fig. 12**
η : Vertical bending amplitude (m)
θ : Torsional amplitude (rad)
$C(k)$: Theodorsen function $\{=F(k)+iG(k)\}$

$$=\frac{H_1^{(2)}(k)}{H_1^{(2)}(k)+iH_0^{(2)}(k)}$$

$F(k)$: Real part of Theodorsen function
$G(k)$: Imaginary part of Theodorsen function
i : Imaginary unit
$H_n^{(2)}(k)$: Hankel function of the first class
k : Reduced frequency (= $\omega b/V$)
ω : Circular frequency (1/s)

These unsteady aerodynamic forces contain a Theodorsen function $C(k)$, which represents the ratio of quasi-steady aerodynamic force to unsteady aerodynamic force. Therefore, the unsteady aerodynamic force lags the quasi-steady aerodynamic force in phase, and this phase lag has a large influence on the flutter characteristics of the plate. From the results of comparison between wind tunnel experiment values and calculated values, it has been reported[14] that there are unreasonable points in applying the above Bleich flutter theory to any suspension bridge. For example, the theoretical value of flutter wind speed is considerably higher than the flutter wind speed obtained from wind tunnel tests. As a major reason for that, because the air flow separates from the stiffened deck cross-section of the suspension bridge, the potential flow assumption fundamental to the flutter theory does not hold true, and therefore the unsteady aerodynamic forces acting on the cross section differ from the theoretical equations of Equations (9) and (10).[15] To find the unsteady aerodynamic forces at the bridge deck cross-section under consideration with high accuracy, direct measurement using a wind tunnel test is mainly used. Recently, computational fluid dynamics (CFD) is strenuously used to calculate unsteady aerodynamic forces in an analytical way.[16]

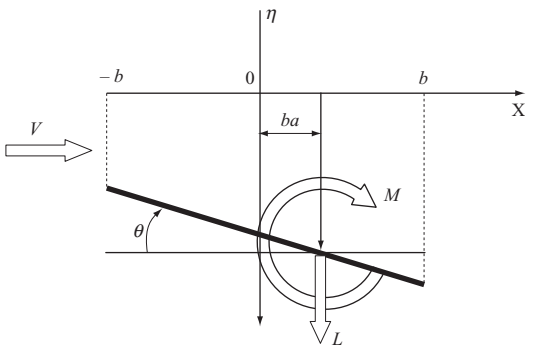

Fig. 12 Aerodynamic forces on oscillating flat plate

This section examines the effects of the Reynolds number on the unsteady aerodynamic forces acting on a bridge deck cross-section of a long-span bridge.

3.2.2 Relationship between Reynolds number and unsteady aerodynamic force coefficients

When a sectional model is in coupled vibration of vertical bending and torsion with a circular frequency ω in a wind of speed V, the unsteady aerodynamic forces acting on the model can be expressed as:

$$D=\pi\rho B^2A_n\omega^2\left\{\left(C_{D\eta R}+iC_{D\eta i}\right)\frac{\eta}{B}+\left(C_{D\theta R}+iC_{D\theta i}\right)\theta\right\} \quad \cdots (11)$$

$$L=\pi\rho B^3\omega^2\left\{\left(C_{L\eta R}+iC_{L\eta i}\right)\frac{\eta}{B}+\left(C_{L\theta R}+iC_{L\theta i}\right)\theta\right\} \quad \cdots\cdots (12)$$

$$M=\pi\rho B^4\omega^2\left\{\left(C_{M\eta R}+iC_{M\eta i}\right)\frac{\eta}{B}+\left(C_{M\theta R}+iC_{M\theta i}\right)\theta\right\} \quad \cdots\cdots (13)$$

where

D : Unsteady drag (N/m)
L : Unsteady lift (N/m)
M : Unsteady pitching moment (N·m/m)
ρ : Air density (kg/m^3)
B : Deck width (m)
A_n : Projected bridge deck area (m^2/m)
ω : Angular frequency (1/s)
η : Vertical bending amplitude (amplitude at center of deck width) (m)
θ : Torsional amplitude (rad)
C_{XYZ} : Unsteady aerodynamic force coefficients (reduced frequency k = function of fB/V, f : frequency, V: mean wind speed)
i : Imaginary unit

For measurement of the unsteady aerodynamic forces acting on a bridge deck, the following two methods are available:

(1) Forced oscillation method
This method was developed by Kawashima et al.[17] and applied to a suspension bridge model by Ukeguchi and Sakata.[18), (19)] Unsteady aerodynamic forces are measured while the model is in forced oscillation.

(2) Free oscillation method
While a two-dimensional rigid model is set in free oscillation in an air flow, the response frequency, response logarithmic decrement, amplitude ratio of vertical bending to torsional motion and phase difference are measured. The unsteady aerodynamic forces are calculated back.[20]

In this study, the unsteady aerodynamic forces were measured by the forced oscillation method. This measuring method is based on the assumption that the bridge deck should be in harmonic oscillation when it flutters. Therefore, the unsteady aerodynamic force coefficients obtained by the forced oscillation method may depend on amplitude. An investigation into the amplitude dependence is described in **Section 3.2.3**.

Measured results of unsteady aerodynamic forces[21), (22)] are shown in **Figs. 13** to **16**. Vertical axis represents the unsteady aerodynamic force coefficients according to the definition equations shown as Equations (12) and (13). Horizontal axis represents reduced frequency $k = fB/V$ (f : frequency, B: deck width, V: mean wind speed). In these figures, the Theodorsen function is also shown for comparison. The unsteady drag coefficient is not shown because it has little influence on the flutter of the bridge with box girder.[23]

Of the measured unsteady aerodynamic coefficients at Deck section A and at an angle of attack of 0 degree shown in **Fig. 13**, the coefficients $C_{M\eta i}$ and $C_{L\theta R}$[24), (25)] having a large influence on flutter, hardly showed a discernible change with the Reynolds number. The coefficient that showed a large change with Reynolds number was $C_{L\theta i}$. As the dependence on Reynolds number, the value of this coefficient becomes negative for a Reynolds number of 9.5×10^4 or less, while it becomes positive for 3.4×10^5 or more. However, the effect of this coefficient on flutter characteristics is said to be small. Comparing the measured unsteady aerodynamic force coefficients with the Theodorsen function, the two show about the same tendency, though they differ in magnitude.

Of the measured unsteady aerodynamic coefficients at Deck section A and at an angle of attack of +3 degrees shown in **Fig. 14**, the coefficients influenced greatly by Reynolds number are $C_{M\eta R}$, $C_{M\eta i}$, $C_{M\theta R}$ and $C_{M\theta i}$ related to the pitching moment. That is, $C_{M\theta i}$ having a large influence on flutter is included in those coefficients. On the other hand, $C_{L\theta R}$ has a large influence on flutter; however, no dependence on Reynolds number is seen. Considering the measured results in this case and the above results at an angle of attack of 0 degree, it was found that at different angles of attack, different unsteady aerodynamic force coefficients have a dependence on Reynolds number even for the same bridge deck cross-section shape.

Figures 15 and **16** show the measured unsteady aerodynamic force coefficients at sections B and C, and they

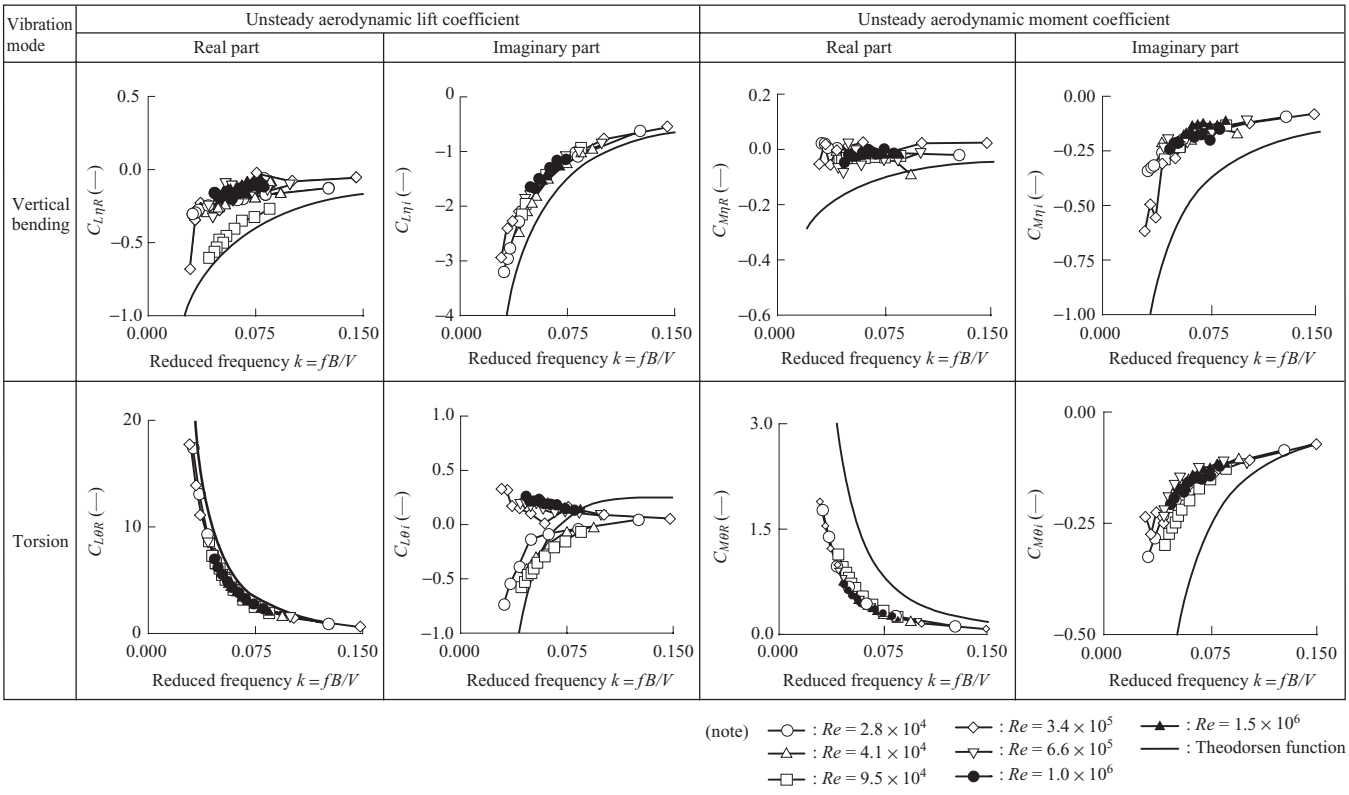

Fig. 13 Unsteady aerodynamic force coefficients (Deck section A, Angle of attack : α = 0 degree)

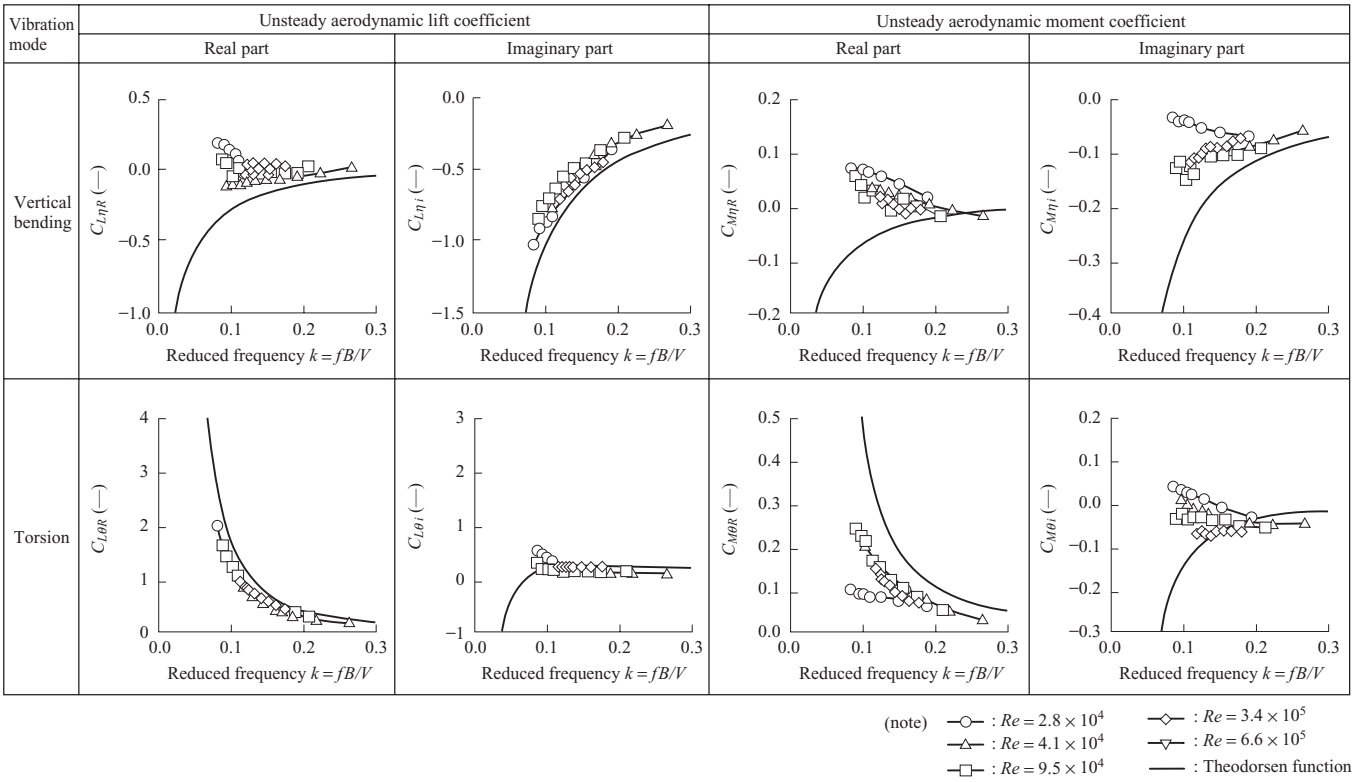

Fig. 14 Unsteady aerodynamic force coefficients (Deck section A, Angle of attack : α = +3 degrees)

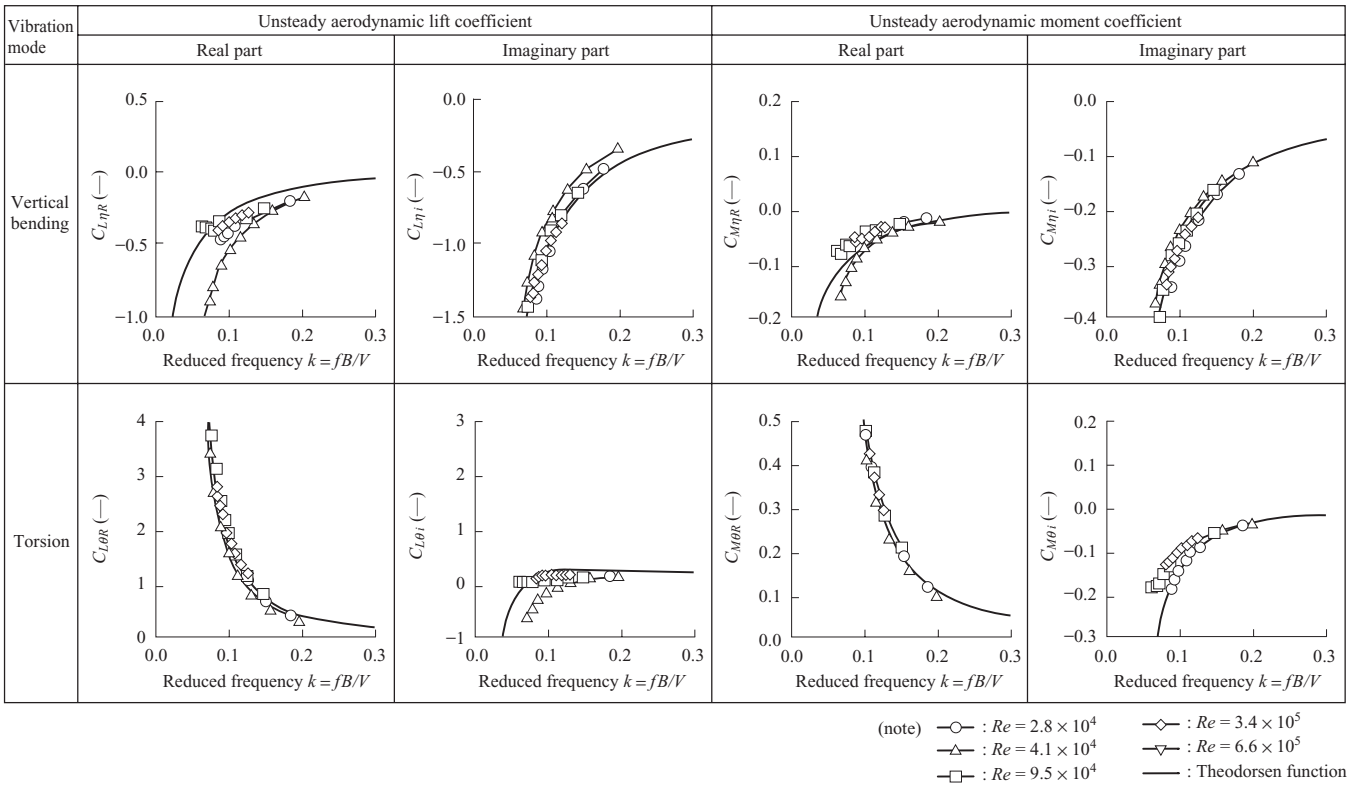

Fig. 15 Unsteady aerodynamic force coefficients (Deck section B, Angle of attack : α = +3 degrees)

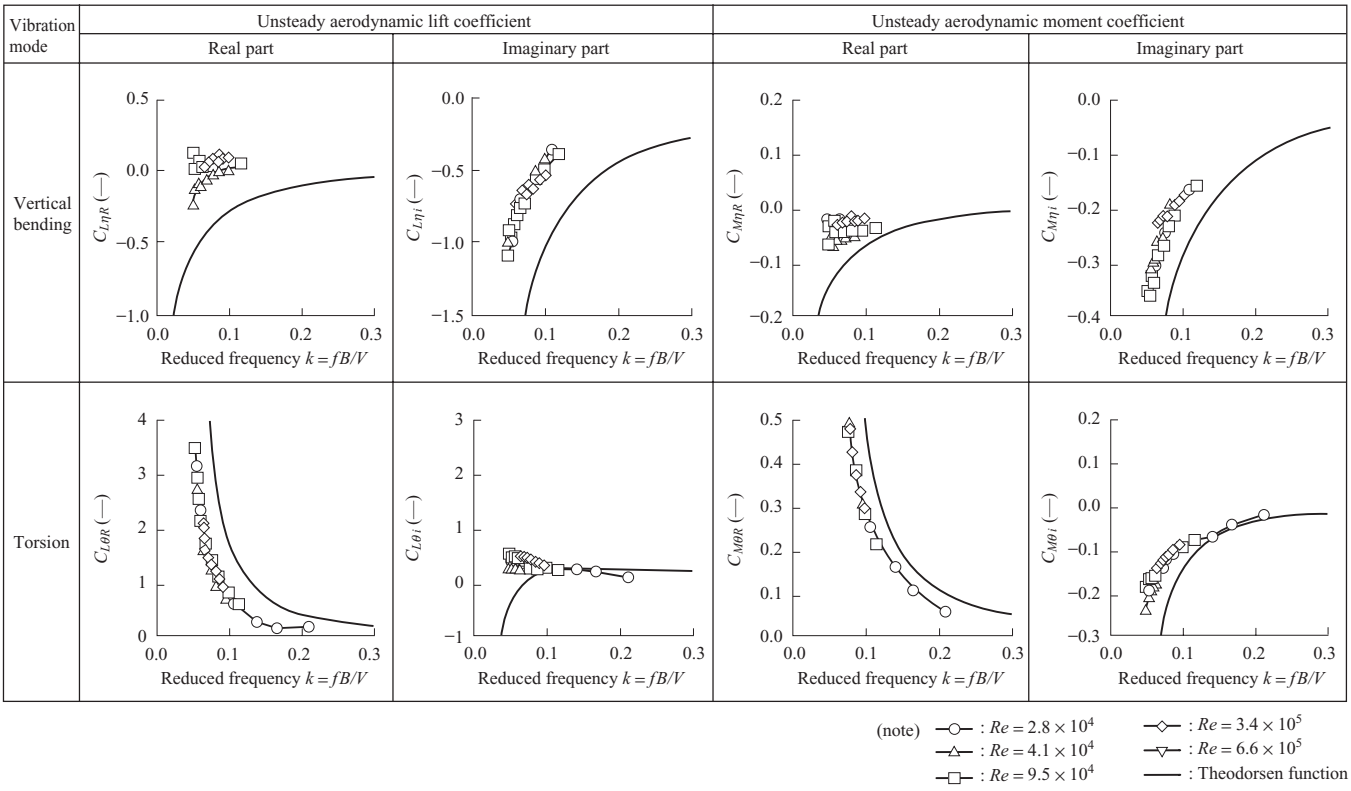

Fig. 16 Unsteady aerodynamic force coefficients (Deck section C, Angle of attack : α = +3 degrees)

are qualitatively similar to the Theodorsen function, and no dependence on the Reynolds number is seen. As a reason for this, it is thought that this is because these sections have a shape closer to a thin plate than Deck section A.

Of the unsteady aerodynamic force coefficients at Deck section A and angle of attack of +3 degrees in which Reynolds number effects were seen in **Fig. 14**, $C_{M\theta R}$ and $C_{M\theta i}$ are the aerodynamic moment coefficients accompanied by torsional excitation. Paying attention to these coefficients, the mechanism of Reynolds number effects is investigated from the measured results of fluctuating pressure distribution at the model surface.

The fluctuating pressure distribution at the model surface was measured for three different Reynolds numbers, and the results are shown in **Fig. 17**. As the Reynolds number increases, the fluctuating pressure peak on the bottom surface of the upstream deck half shifts upstream. It can be thought that the magnitudes of $C_{M\theta R}$ and $C_{M\theta i}$ in **Fig. 14** increase with the Reynolds number for this reason. The tendency of the pressure distribution at the model surface changing with the Reynolds number was seen in **Fig. 9**, or in the mean pressure distribution measured when the model was at rest. As shown in **Fig. 17**, it was found that the same tendency is seen in the fluctuating pressure distribution when the model is excited.

3.2.3 Amplitude dependence of unsteady aerodynamic force coefficients

In general, the unsteady aerodynamic force coefficients are not necessarily linear with respect to amplitude, and

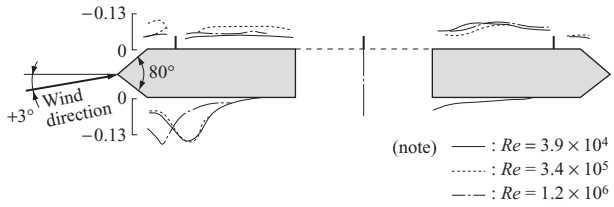

Fig. 17 Unsteady pressure coefficients : C_{PD} (Deck section A, α = +3 degrees, θ = 1 degree)

nonlinearity may have influence on the flutter response characteristics, depending on the circumstances. However, flutter analysis ordinarily performed is premised on the condition that the unsteady aerodynamic force coefficients are linear. Therefore, it is desirable to change the amplitude to see whether the unsteady aerodynamic force coefficients have amplitude dependence or not.[26), (27)]

As a past study on amplitude dependence, unsteady aerodynamic forces of "the Great Belt East Bridge," Denmark, were measured using a 1/300-scale taut strip model having a flattened hexagonal cross-section.[28)] It is reported that no amplitude dependence was observed at a reduced wind speed $V_r = V/fB$ (V: mean wind speed, f : frequency, B: deck width) of 10 or less, and some measure of amplitude dependence was observed at more than 10. It must be noted, however, that the Reynolds number in this study is, taking the deck height D as the representative length, as small as $Re = VD/\nu = 6.5 \times 10^3$ (V: mean wind speed = 6.5 m/s, D : deck height = 4.4 m/300 = 0.014 7 m,

v : kinematic viscosity = 1.46×10^{-5} m^2/s.

In this study, Reynolds number dependence was observed at Deck section A and an angle of attack of +3 degrees, so the amplitude dependence of unsteady aerodynamic force coefficients was investigated in this condition by changing the oscillation amplitudes of vertical bending and torsion. For the model, a 1/10-scale bridge deck sectional model was used. For the oscillation amplitude, a vertical bending amplitude $\eta_m = B_m/100$ (B_m : model deck width) and torsional amplitude $\theta = 1.0$ degree in the Wind Tunnel Test Specification[29] were taken as reference, and a total of three sets of values, including one third and two thirds of these values, were used. It is important to grasp the unsteady aerodynamic force coefficient characteristics at small amplitudes because they have influence from the initial state of flutter. Thus, these smaller amplitudes than the reference were chosen. Measured results are shown in **Fig. 18**. In any measured unsteady aerodynamic force coefficient, no significant difference due to different oscillation amplitudes was observed. In a high Reynolds number region which is smaller by a factor of 10^1 than the Reynolds number of a real bridge, no amplitude dependence of unsteady aerodynamic force coefficients was observed. From this, the vertical bending amplitude $\eta_m = B_m/100$ and the torsional amplitude $\theta = 1$ degree stipulated in the Wind Tunnel Test Specification are thought to be valid.

4. Wind-induced response analysis of real bridge

Here, the steady and unsteady aerodynamic force coefficients obtained in **Section 3** are applied to a full bridge model of a long-span bridge, and static displacement analysis and flutter analysis in strong winds are performed. By this, the effects of the Reynolds number on the static displacement under wind load and flutter characteristics are investigated.

4.1 Wind-induced static displacement analysis

4.1.1 Analysis model and method

The long-span bridge analyzed is a 3-span, 2-hinge stiffened box girder suspension bridge with a main span of 2 500 meters. Its structural dimensions are shown below.

Suspension structure type
: 3-span, 2-hinge stiffened box girder suspension bridge

Span divisions
- Cable: 1 250 m + 2 500 m + 1 250 m
- Deck: 1 226 m + 2 480 m + 1 226 m
- Sag ratio: 1/10

Cable
- Tension: 586 289 kN
- Cable-to-cable distance: 35.5 m
- Diameter: 1.324 m
- Cross-sectional area: 0.871 m^2 per cable

Mass per unit length
- Stiffening girder: 23.09 t/m (uniform over all spans)
- Cable: 7.66 t/m per cable (uniform over all spans)
- Suspension structure: 38.41 t/m per bridge

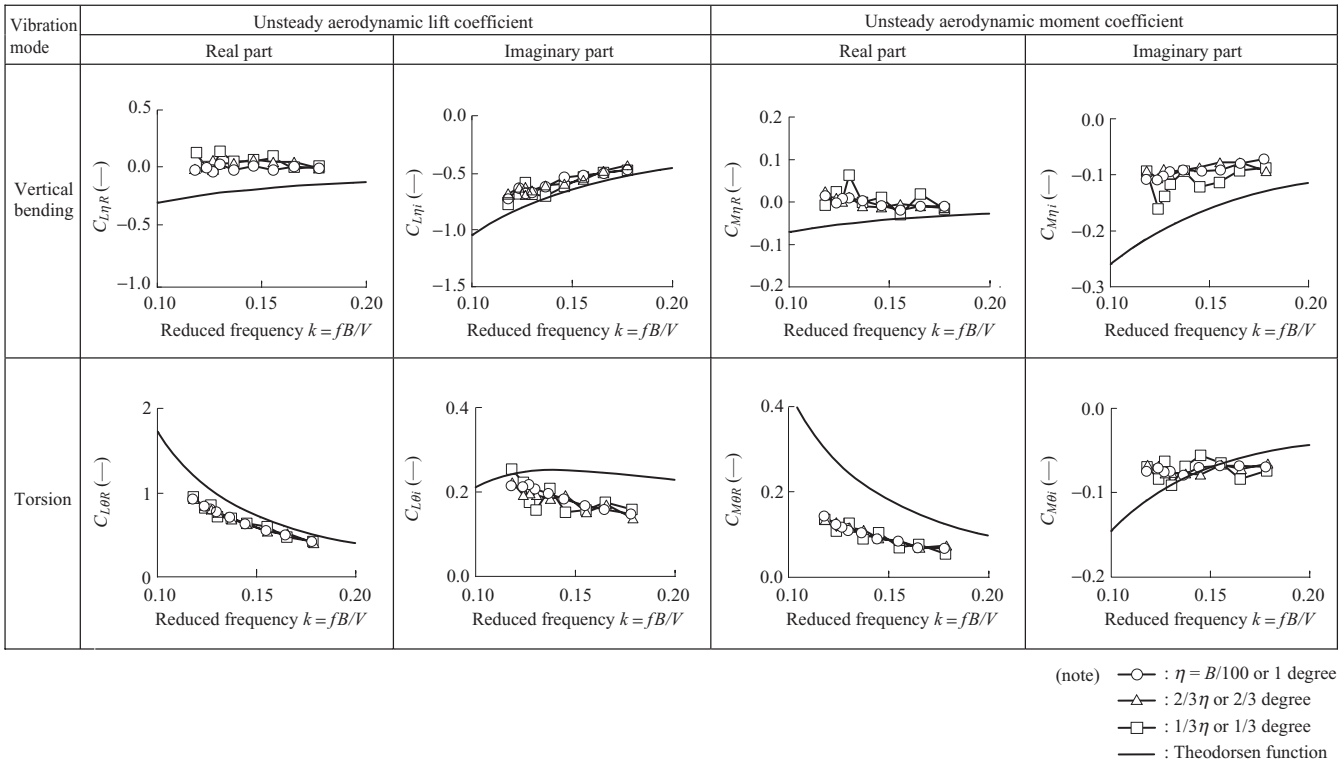

Fig. 18 Amplitude effects on unsteady aerodynamic force coefficients (Deck section A, α = +3 degrees)

(uniform over all spans)

Polar moment of inertia per unit length

Stiffening girder 2 712 t·m^2/m (uniform over all spans)

Cable 4 827 t·m^2/m per cable (uniform over all spans)

Suspension structure 7 539 t·m^2/m per bridge (uniform over all spans)

Section properties

Cross-sectional area 1.314 m^2 (uniform over all spans)

Vertical bending rigidity 3.837 m^4 (uniform over all spans)

Horizontal bending rigidity 146.4 m^4 (uniform over all spans)

Torsional rigidity 9.700 m^4 (uniform over all spans)

The analysis model is an FEM analysis model of a solid framework. The bridge deck and cable members were divided into 20 parts in the main span and 10 parts in the side spans, giving consideration to ensuring that significant natural oscillation modes could be reproduced in flutter analysis. A schematic of the long-span bridge analysis model is shown in **Fig. 19**.

The wind-induced static displacements were analyzed using the finite element structural analysis program AERODYNA[30] - [32] developed by IHI. This program is capable of finite displacement analysis including wind load imposition, removal or addition of structural members and other shape change history of the structure. Using a method that increases load on a step-by-step incremental basis,[33] a wind load equivalent to a wind speed of 70 m/s was divided into 10 equal parts and successively imposed on the structural members of the bridge deck, main towers, cables and hangers of the analysis model. The bridge deck's steady aerodynamic force coefficients used for the analysis are the wind tunnel test values measured at different Reynolds numbers as shown in **Fig. 6**. For the main towers, cables and hangers, the steady aerodynamic force coefficients in the Wind Resistant Design Code for Honshu-Shikoku Bridges[34] were used.

4.1.2 Analysis results

Figure 20 shows the results of the wind-induced static

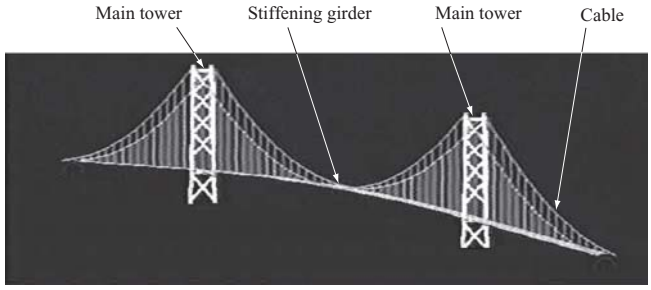

Fig. 19 Analytical model

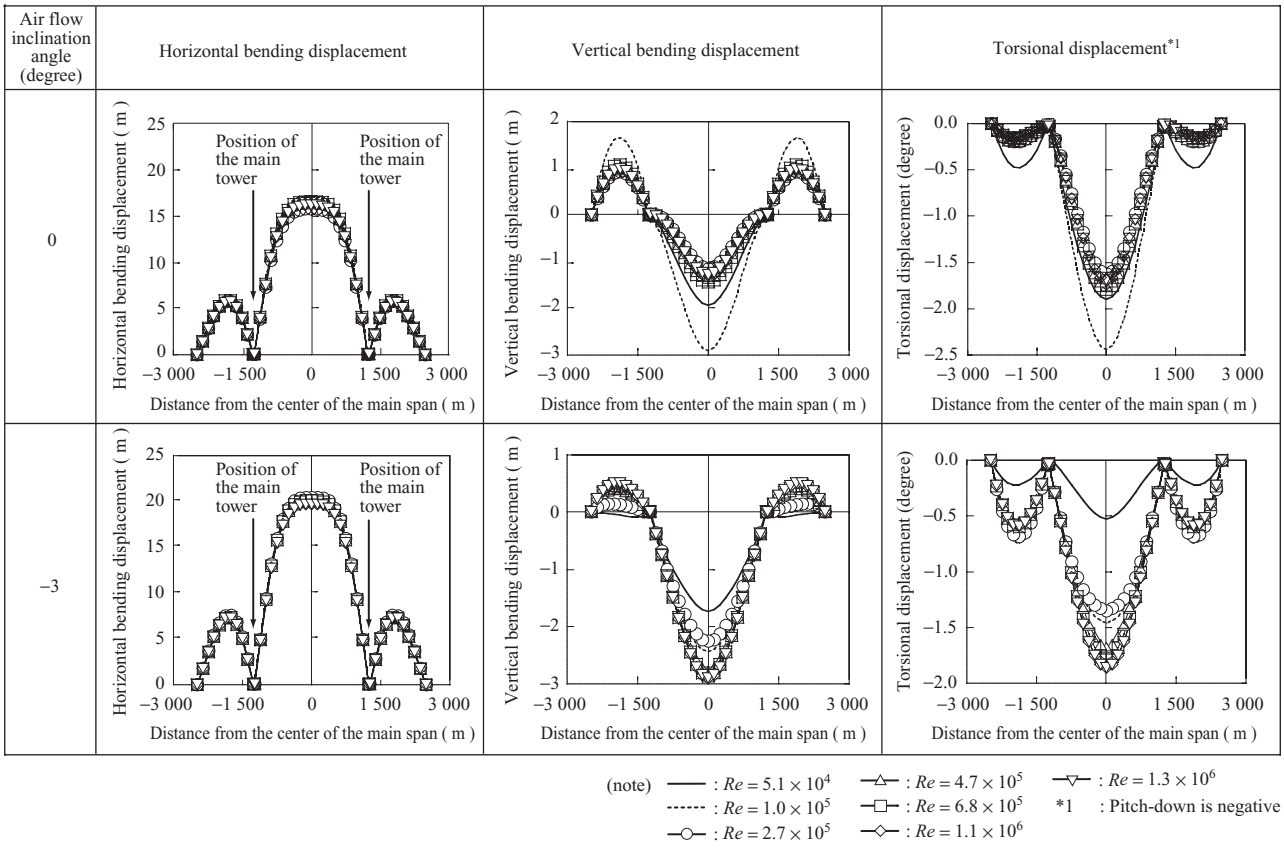

Fig. 20 Wind-induced static deformations at a wind speed of 70 m/s at deck height (Inclination angle : 0 degree and -3 degrees)

displacement analysis of a stiffening girder. It can be seen that the horizontal bending displacement is not influenced by the Reynolds number. This is ascribable to the fact that the drag coefficient is hardly influenced by the Reynolds number in **Fig. 6**. On the other hand, the vertical bending displacement and torsional displacement are influenced by the Reynolds number. That is, at an air flow inclination angle of 0 degree, the results of analysis using the steady aerodynamic force coefficients at a low Reynolds number tend to show a larger displacement than the results of analysis using the coefficients in the high Reynolds number region. This is due to the fact that, as shown in **Fig. 6**, the lift and moment coefficients in the low Reynolds number region are negative and their magnitudes are large in the range of angle of attack from −2.5 to 0 degrees. At an air flow inclination angle of −3 degrees, the results of analysis using the steady aerodynamic force coefficients in the low Reynolds number region contrariwise tend to show a smaller displacement than the results using the coefficients in the high Reynolds number region. This is ascribable to the fact that, as shown in **Fig. 6**, the lift and moment coefficients in the low Reynolds region are negative and their magnitudes are small in the range of angle of attack from −5 to −3 degrees.

As stated above, it was found that the horizontal bending displacement of a long-span suspension bridge is hardly influenced by the Reynolds number. Therefore, even if a static wind-resistant design is done using the drag coefficient obtained by a wind tunnel test in a low Reynolds number region, its results are thought to be valid as a wind-resistant design. On the other hand, it was found that the vertical bending and torsional displacements are influenced by the Reynolds number. Thus, for the vertical bending and torsional displacements, analysis should be performed using steady aerodynamic coefficients obtained in a high Reynolds number region as close as possible to the real bridge.

This also affects the analysis accuracy of aerodynamic stability of a long-span bridge in a strong wind. That is, the vertical bending displacement of the bridge deck contributes to the vertical bending rigidity of the whole suspension bridge system and thereby affects the calculation of the natural frequencies and natural oscillation modes of the whole suspension bridge system in a strong wind. As to torsional displacement, the unsteady aerodynamic force coefficient characteristics may depend on the angle of attack when doing flutter analysis, so it is very important to evaluate this torsional displacement with high accuracy.

4.2 Flutter analysis

4.2.1 Analysis model and techniques

The analysis model is the same as the one used for the wind-induced static displacement analysis in the previous section. An eigenvalue analysis was performed in the state under static wind load, and the values obtained first to the 50th natural frequencies and natural oscillation modes were used for the analysis. For the flutter analysis, a technique based on the modal analysis method[35] was employed. For the unsteady aerodynamic force coefficients, the values shown in **Fig. 13** were used.

4.2.2 Analysis results

Figure 21 shows the results of real bridge flutter analysis.[21), (36)] Up to a Reynolds number of 0.8×10^6, the flutter wind speed was about 70 m/s independent of the Reynolds number. At higher Reynolds numbers, however, the flutter wind speed somewhat increased. This tendency of flutter wind speed's increasing from a Reynolds number of 1.0×10^6 is the same as the results of a flutter analysis[22] performed on a structural system in a spring-supported test and using an analysis model. The latter is the analysis result at an angle of attack of +3 degrees and the analysis results in **Fig. 21** are in the case of an air flow inclination angle (angle of attack) of 0 degree. As above, although the unsteady aerodynamic force coefficients used for analysis were different, Reynolds number effects on flutter wind speed showed the same tendency not dependent on angle of attack.

That is, because the flutter wind speed shows a rising tendency from a Reynolds number of 1.0×10^6 and an ordinary flutter check is done by a wind tunnel test or flutter analysis in a low Reynolds number region of the order of 10^4 to 10^5, such a check is thought to give an evaluation on the safe side in the wind-resistant design. However, this is a conclusion restricted to the bridge deck cross-sections taken up in this study.

5. Conclusion

As a result of the wind tunnel test and wind-induced response analysis performed in this study, the following findings were obtained. Note, however, that these findings are restricted to the bridge deck cross-sections investigated in this study.

(1) A flutter analysis performed using the unsteady

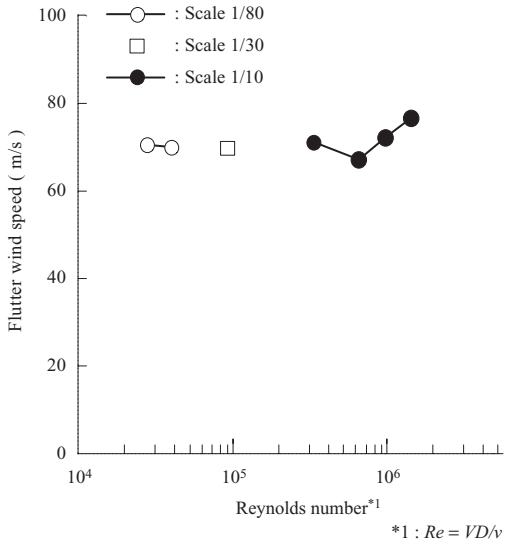

Fig. 21 Flutter analysis results using a three-dimensional analytical model with a main span of 2 500 m (Inclination angle : 0 degree)

aerodynamic coefficients obtained in an ordinary low Reynolds number region gives an evaluation on the safe side in the wind-resistant design.

(2) Because no amplitude dependence of unsteady aerodynamic coefficients was observed in a high Reynolds number region which is smaller by a factor of 10^1 than the Reynolds number of a real bridge, the reference amplitude in Wind Tunnel Test Specification for Honshu-Shikoku Bridges (2001) is valid.

The tasks for the future include measurement and investigation of the steady and unsteady aerodynamic force characteristics in a turbulent flow in a high Reynolds number region.

— Acknowledgments —

The authors sincerely thank Prof. Hiroshi Tanaka at the University of Ottawa, Mr. Kevin Cooper, a former NRC Senior Research Officer, Prof. Hitoshi Yamada at Yokohama National University Graduate School, Prof. Hiromichi Shirato at Kyoto University Graduate School and Prof. Kichiro Kimura at Kyushu Institute of Technology Graduate School for their generous advice and cooperation in the implementation of this study.

REFERENCES

(1) Subcommittee on Similarity of Wind Tunnel Experiments : Is a bridge oscillating due to winds? Subcommittee on Similarity of Wind Tunnel Experiments(the second period), Proceedings of the workshop of subcommittee on Similarity of Wind Tunnel Experiments(the second period) July 1996 pp. 60-61

(2) G. Schewe and A. Larsen : Reynolds number effects in the flow around a bluff bridge deck cross section, Journal of Wind Engineering and Industrial Aerodynamics 74-76 (1998) pp. 829-838

(3) C. Barre and G. Barnaud : High Reynolds number simulation techniques and their application to shaped structures model test, Proceedings of the 1st IAWE European and African Regional Conference on Wind Engineering Guernsey UK (1993) pp. 83-93

(4) M. C. H. Hui and A. Larsen : Aerodynamic investigation for the deck of Stonecutters Bridge emphasizing Reynolds number effects, Proceedings of the 2nd International Symposium on Advances in Wind & Structures (AWAS '02) Busan Korea (2002) pp. 649-656

(5) G. L. Larose, S. V. Larsen, A. Larsen, M. Hui and A. G. Jensen : Sectional model experience at high Reynolds number for the deck of a 1 018 m span cable-stayed bridge, Proceedings of 11th International Conference on Wind Engineering Lubbock Texas USA (2003) pp. 373-380

(6) G. Schewe : Reynolds number effects in flow around more-or-less bluff bodies, Journal of Wind Engineering and Industrial Aerodynamics 89 (2001) pp. 1 267-1 289

(7) U.Y. Jeong, H. M. Koh and H. S. Lee : Finite element formulation for the analysis of turbulent wind flow passing bluff structures using the RNG k-ε model, Journal of Wind Engineering and Industrial Aerodynamics 90 (2002) pp. 151-169

(8) P. W. Bearman : On vortex shedding from a circular cylinder in the critical Reynolds number regime, Journal of Fluid Mechanics 37 part 3 (1969) pp. 577-585

(9) G. Schewe : On the force fluctuation acting on a circular cylinder in crossflow from subcritical up to transcritical Reynolds numbers, Journal of Fluid Mechanics 133 (1983) pp. 265-285

(10) K. Matsuda and S. Zan : Aerodynamic characteristics of 2-dimensional circular cylinders at high Reynolds numbers, Proceedings of the 33rd Fluid Dynamics Conference Sep. 2001

(11) K. Shu, Y. Kubo, T. Hironaka and K. Tazaki : Reynolds number effects on Strouhal number of bluff structures, Proceedings of JSCE West Division Annual Meeting(I)-47 March 1992 pp. 114-115

(12) F. Bleich : Dynamic instability of truss-stiffened suspension bridges under wind action, Trans. American Society of Civil Engineers 114 (1949)

(13) T. Theodorsen : General theory of aerodynamic instability and the mechanism of flutter, NACA TR 496 (1935) pp. 413-433

(14) F. Kaneko : Numerical Study of the FLUTTER Theory for Aerodynamic Stability of Long Span Suspension Bridges, Ishikawajima-Harima Engineering Review Vol.2 No.4 Jan. 1962 pp. 69-83

(15) H. Tanaka and M. Ito : The characteristics of the aerodynamic forces in self-excited oscillations of bluff structures, Journal of Structural Mechanics and Earthquake Engineering, JSCE, No.168 Aug. 1969 pp. 15-24

(16) See, for example, S. Kuroda : Numerical computation of unsteady aerodynamic forces for long-span bridge with two-equation turbulence model, Journal of Structural Mechanics and Earthquake Engineering, JSCE No.654/(I)-52 July 2000 pp. 377-387

(17) S. Kawashima, H. Kimura and T. Shibato : An experiment for unsteady aerodynamic forces acting on a wing, Proceedings of 13th Japan National Congress for Applied Mechanics Sep. 1963 pp. 19-20

(18) N. Ukeguchi and H. Sakata : An investigation of aeroelastic instability of suspension bridge, Journal of JSASS / Journal of the Japan Society for Aeronautical and Space Science Vol.133 Feb.1965 pp. 27-36

(19) N. Ukeguchi, H. Sakata and H. Nishitani : An investigation of aeroelastic instability of suspension

bridges, International Symposium on Suspension Bridges Laboratorio Nacional de Engenharia Civil Lisbon (1966) pp. 273-284
(20) R. H. Scanlan : Airfoil and bridge deck flutter derivatives, Journal of Engineering Mechanics Division, Proceedings of the American Society of Civil Engineering 97 EM6 Dec. 1971 pp. 1 717-1 737
(21) K. Matsuda, K. R. Cooper and H. Tanaka : The analysis of wind-induced static displacements and flutter for long-span suspension bridges using steady and unsteady aerodynamic forces measured at high Reynolds numbers, Proceedings of 11th International Conference on Wind Engineering, Lubbock Texas USA (2003) pp. 649-656
(22) K. Matsuda, K. R. Cooper, H. Tanaka, M. Tokushige and T. Iwasaki : An investigation of Reynolds number effects on the steady and unsteady aerodynamic forces on a 1:10 scale bridge deck section model, Journal of Wind Engineering and Industrial Aerodynamics 89 (2001) pp. 619-632
(23) Y. Hikami and K. Matsuda : On the characteristics of unsteady aerodynamic forces on flutter of long-span bridges, Proceedings of the 50th JSCE Annual Meeting (I)-687 Sep. 1995 pp. 1 374-1 375
(24) M. Matsumoto, Y. Kobayashi and H. Hamasaki : On mechanism of coupled flutter for fundamental bluff bodies, Proceedings of the 13th National Symposium on Wind Engineering Nov. 1994 pp. 359-364
(25) M. Matsumoto, Y. Daito, F. Yosizumi, Y. Ichikawa and T. Yabutani : Torsional flutter of bluff bodies, Journal of Wind Engineering and Industrial Aerodynamics 69-71 (1997) pp. 871-882
(26) Y. Kubo, M. Ito and T. Miyata : Nonlinear analysis of aerodynamic response of suspension bridges in wind, Journal of Structural Mechanics and Earthquake Engineering, JSCE No.252 1976 pp. 35-46
(27) H. Yamada, T. Miyata, H. Katsuchi, T. Suzuki and H. Sugiura : A study on non-linear extension of unsteady aerodynamic force definition, Journal of Structural Engineering Vol.47A March 2001 pp. 967-976
(28) G. L. Larose, A. G. Davenport and J. P. C. King : On the unsteady aerodynamic forces on a bridge deck in turbulent flow, Proceedings of the 7th US National Conference on Wind Engineering UCLA USA (1993)
(29) Honshu-Shikoku Bridge Authority: Wind Tunnel Test Specification for Honshu-Shikoku Bridges (2001) Aug. 2001
(30) T. Yuki and K. Ando : Studies on Finite Element Method for Structural Analysis - 4th Report Analysis of Vibration, Buckling and Large Deformation for Framed Structure -, Ishikawajima-Harima Engineering Review Vol.10 No.4 July 1970 pp. 327-336
(31) T. Yuki, T. Shimada and Y. Hikami : Studies on Finite Element Method for Structural Analysis - Large Deformation Structure Analsysis Program for Suspension Bridge and Plane Frame - , IHI Engineering Review Vol.6 No.2 Sep. 1973 pp. 24-29
(32) K. Matsuda, H. Uejima, M. Tokushige and T. Iwasaki : Numerical Computation for Aeroelastic Stability of Long-Span Bridges, Ishikawajima-Harima Engineering Review Vol.37 No.6 Nov. 1997 pp. 411-417
(33) Y. Hikami, K. Matsuda and T. Suzuki : Nonlinear geometric and aerodynamic analysis for a long-span cable-stayed bridge during construction, Wind Engineering Proceedings of the 1st IAWE European and African Regional Conference Guernsey UK (1993) pp. 431-440
(34) Honshu-Shikoku Bridge Authority: Wind Resistant Design Standard for Honshu-Shikoku Bridges (2001) Aug. 2001
(35) T. J. A. Agar : Aerodynamic flutter analysis of suspension bridge by a modal technique, Engineering Structure Vol.11 April 1989 pp. 75-82
(36) K. Matsuda, K. R. Cooper and H. Tanaka : Reynolds number effects on wind-induced static displacements and flutter for long-span suspension bridges, Journal of Wind Engineering, JAWE, No.95 April pp. 109-110